Flavonoid O-methytransferases in *Eucalyptus* – Biosynthesis of Alpinetin via a Methylated Chalcone Precursor

Liyuan Zhu [†], Guillermo Garcia-Gimenez [†], John Humphries, Adam W.E. Stewart, Spencer J. Williams, Jason Q.D. Goodger [*]

Posted Date: 1 May 2026

doi: 10.20944/preprints202604.2208.v1

Keywords: cardamomin; cardamonin; enzyme regioselectivity; flavone; monocalypt; natural products; SAM-dependent methyltransferase

 doi:10.20944/preprints202604.2208.v1

Article

Flavonoid O-methytransferases in *Eucalyptus* – Biosynthesis of Alpinetin via a Methylated Chalcone Precursor

Liyuan Zhu [1,†], Guillermo Garcia-Gimenez [1,†], John Humphries [2], Adam W.E. Stewart [3], Spencer J. Williams [3] and Jason Q.D. Goodger [1,*]

[1] School of Agriculture, Food and Ecosystem Sciences, University of Melbourne, Parkville, Victoria, Australia 3010

[2] La Trobe Institute for Sustainable Agriculture & Food, La Trobe University, Bundoora, Victoria, Australia 3086

[3] School of Chemistry and Bio21 Molecular Science and Biotechnology Institute, University of Melbourne, Parkville, Victoria, Australia 3010

* Correspondence: jgoodger@unimelb.edu.au

† These authors contributed equally to this work.

Abstract

Methylated flavonoids are abundant phytochemicals in *Eucalyptus* and are of interest because methylation can alter flavonoid diversity, bioactivity and stability. The enzymes responsible for flavonoid methylation in eucalypts are largely uncharacterised. We used comparative leaf transcriptomics of two species with contrasting flavanone profiles, together with protein-structure-guided candidate selection, to identify prospective *O*-methyltransferases (OMTs) involved in methylated flavonoid biosynthesis. Five candidate OMTs from *E. eugenioides* were cloned, heterologously expressed and assayed against a panel of flavonoids and a chalcone precursor. The enzymes showed distinct substrate preferences and regioselectivities. *Ee*OMT1 acted as a broad 7-*O*-methyltransferase, whereas *Ee*OMT3–*Ee*OMT5 preferentially methylated B and C-ring hydroxyl groups, with differing capacities for sequential methylations at different sites. *Ee*OMT2 was of particular interest because it effectively methylated pinocembrin chalcone to alpinetin chalcone, while only weakly converting pinocembrin to alpinetin. Expression–metabolite analyses across *E. eugenioides* genotypes supported roles relating to *in planta* accumulation of 5-*O*- and 7-*O*-methylated flavanones, for *Ee*OMT2 and *Ee*OMT1, respectively. These findings support a revised model in which alpinetin biosynthesis proceeds, at least in part, through methylation of a chalcone precursor before flavanone formation. This provides a foundation for elucidating flavonoid methylation pathways and for engineering tailored methylated flavonoids for industrial applications.

Keywords: cardamomin; cardamonin; enzyme regioselectivity; flavone; monocalypt; natural products; SAM-dependent methyltransferase

1. Introduction

Flavonoids are chemically diverse specialized metabolites with a range of physiological roles in plants including UV photoprotection and pathogen defence [1–3]. Many have antioxidant and anti-inflammatory activities relevant to food, nutraceutical and pharmaceutical applications [4–7]. The flavonoid skeleton is produced through the phenylpropanoid biosynthetic pathway, and their structural and functional diversity is explained by enzymatic tailoring reactions, including methylation, glycosylation and acylation [8]. Flavonoid methylation is catalysed by *S*-adenosyl-L-methionine (SAM)-dependent *O*- and/or *C*-methyltransferases (OMTs and CMTs; [9]), and can alter

 doi:10.20944/preprints202604.2208.v1

their metabolic stability and resistance to enzymatic degradation, thereby improving their therapeutic potential [10–12].

Eucalyptus trees (>800 species [13]; Family Myrtaceae) are rich sources of methylated flavonoids, including *O*- and *C*-methylated flavanones and flavones [14–17]. In monocalypt eucalypts (species of subgenus *Eucalyptus*), methylated flavanones accumulate in leaf surface waxes and in the terpenic oils housed within copious foliar oil glands [18,19]. These flavonoid profiles are often species- or genotype-specific, providing a useful system for linking chemical variation with candidate biosynthetic genes.

Plant OMTs that methylate flavones and flavonols have been relatively well characterised and often show defined regioselectivity patterns [20–23]. By contrast, flavanone OMTs have not been as well studied. A flavanone 7-OMT from *Eucalyptus nitida* (*En*OMT1) was recently shown to convert the non-methylated flavanone pinocembrin to the 7-*O*-methylated flavanone pinostrobin [24]. A plant enzyme responsible for formation of the 5-*O*-methylated pinocembrin derivative alpinetin – an important pharmacological component of many traditional Chinese medicines and patent drugs [25] – has not yet been characterized. Although engineered bacterial OMTs can methylate the 5-hydroxyl of pinocembrin to generate alpinetin in a reasonable yield, the low catalytic activity and yield (<10%) of the wild-type enzyme suggests that direct methylation of a flavanone precursor may not be a preferred route to this product in plants [26].

An alternative possibility is that methylation occurs on a chalcone precursor, before flavanone ring closure. Recent work on methylated flavonoids in *Rhododendron dauricum* showed that *C*-methylation can occur on a precursor chalcone, followed by isomerisation into the corresponding methylated flavanone [27]. Thus, the ongoing search for an OMT involved in alpinetin should consider pinocembrin chalcone as a potential substrate for OMT activity.

In this study, we used comparative transcriptomics of eucalypts with contrasting flavanone profiles, together with protein modelling and recombinant enzyme assays, to identify five candidate OMTs involved in methylated flavonoid biosynthesis. By testing both flavanone and chalcone precursors, we investigated whether alpinetin formation proceeds through direct methylation of pinocembrin or through methylation of pinocembrin chalcone before flavanone formation. The results identify *Ee*OMT2 as a candidate chalcone OMT and support a revised route to alpinetin and related 5-*O*-methylated flavanones via methylation of a chalcone precursor.

2. Results

2.1. Variation in Flavanone Abundance and Diversity Between Eucalypts

Two monocalypt eucalypts, *Eucalyptus eugenioides* (thin-leaved stringybark) and *E. stenostoma* (Jillaga ash), were selected for analysis based on their contrasting foliar flavanone profiles. *Eucalyptus eugenioides* accumulated a higher total flavanone content and displayed a more chemically diverse profile, comprising *C*-methylated and 5-*O*-methylated and 7-*O*-methylated flavanones. This included the *C*-methylated flavanones cryptostrobin (36%) and demethoxymatteucinol (3%), the 5-*O*-methylated flavanones alpinetin (16%) and 5-*O*-methyl cryptostrobin (4%), and the 7-*O*-methylated flavanones 7-*O*-methylcryptostrobin (9%), pinostrobin (1%) and 7-*O*-methyldemethoxymatteucinol (1%). The 5-*O*-methylated flavanones 5-*O*-methylcryptostrobin and 7-*O*-methylcryptostrobin were isolated and structurally characterised by single crystal X-ray diffraction (Appendix A1, Figure S1; Table S6). While 7-*O*-methylcryptostrobin has previously been reported from eucalypts [16], this is to our knowledge the first report of 5-*O*-methylcryptostrobin in the genus.

By contrast, *E. stenostoma* contained lower total flavanone levels and a simpler profile dominated by pinocembrin (68%), with alpinetin also present as a significant minor component (13%; Figure 1A). The differences between these two species, particularly in total flavanone abundance and the relative representation of 5-*O*- and 7-*O*-methylated products, provided a basis for comparative transcriptomic analysis aimed at identifying candidate *O*-methyltransferases involved in flavanone methylation.

 doi:10.20944/preprints202604.2208.v1

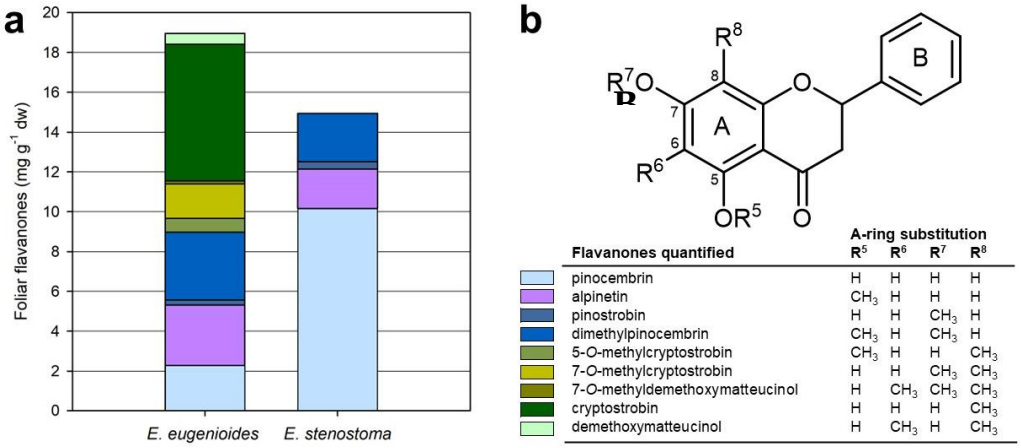

Figure 1. Foliar flavanone profiles of the two eucalypt species selected for comparative transcriptomic analysis. (**a**) Total flavanone content and relative flavanone composition in leaves of *E. eugenioides* and *E. stenostoma*. Values are expressed as mg g^{-1} dry weight. (**b**) General flavanone scaffold showing the positions of observed *O*-methylation (R^5, R^7) and *C*-methylation (R^6, R^8) on the A-ring. The R-group table defines the substitutions corresponding to the flavanones detected in foliar extracts.

2.2. Comparative Transcriptomic Analysis

To investigate foliar transcriptomic differences between *E. eugenioides* and *E. stenostoma*, pairwise differential expression analysis was performed using the *E. grandis* reference genome [28]. This identified more than 19,800 expressed genes. Applying thresholds of p-value < 0.01 and [$\log_2$ (fold change) >1.5] revealed 1,307 genes significantly upregulated in *E. eugenioides* and 890 genes in *E. stenostoma*, corresponding to 7% and 5% of expressed genes, respectively (Figure 2A). Kyoto encyclopedia of genes and genomes (KEGG) pathway enrichment analysis was then performed using the top 1,000 differentially expressed genes to identify biological processes associated with the transcriptomic divergence between species. Pathways were ranked by $-\log_{10}$(false discovery rate; FDR), with higher values indicating stronger enrichment. The most significantly enriched pathway was 'biosynthesis of secondary metabolites' (egr01110; $-\log_{10}$FDR = 7.24). Based on fold enrichment (FE), four of the nine KEGG pathways passing the >1.5-FE cut-off were associated with secondary metabolism, including 'biosynthesis of various plant secondary metabolites' (egr00999; FE = 4.51) and 'flavonoid biosynthesis' (egr00941, FE = 3.99; Figure 2B). Other enriched pathways, including 'tryptophan metabolism', were associated with primary metabolic processes.

Broad pathways such as 'biosynthesis of secondary metabolites' contained the largest number of differentially expressed genes but showed lower FE, whereas more specific pathways generally contained fewer genes and higher FE. This pattern is consistent with targeted regulation of specialised metabolic functions. Inspection of the enriched pathways identified at least 16 putative methyltransferase genes distributed across secondary-metabolism-associated pathways, including 'biosynthesis of secondary metabolites', 'phenylpropanoid biosynthesis' and 'flavonoid biosynthesis' (Table S1).

 doi:10.20944/preprints202604.2208.v1

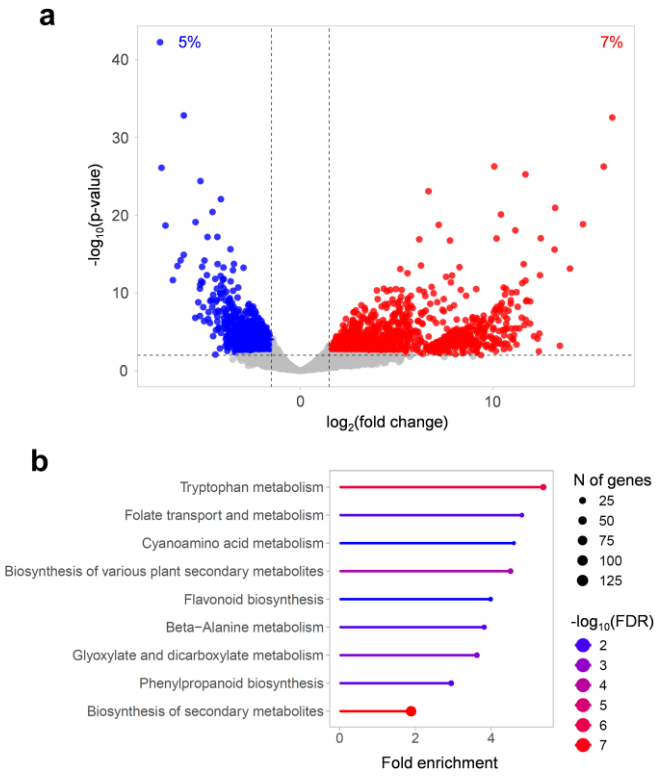

Figure 2. Comparative transcriptomic analysis of eucalypt leaves. (**a**) Volcano plot showing pairwise differential gene expression between *E. eugenioides* and *E. stenostoma*. Red and blue dots indicate genes significantly upregulated in *E. eugenioides* and *E. stenostoma*, respectively; grey dots indicate genes that did not meet the significance thresholds. Dashed lines show the applied cut-offs (*p*-value < 0.01 and $\log_2$FC >1.5 or <-1.5). The percentage of significantly upregulated genes in each species is shown above the corresponding wing of the volcano plot. (**b**) KEGG analysis of the top 1,000 differentially expressed genes (DEGs). The nine most enriched pathways passing the >1.5-FE threshold are shown. Bubble size indicates the number of DEGs assigned to each pathway, FE indicates enrichment relative to the background gene set (*n* = 19,878), and colour indicates statistical significance, expressed as -$\log_{10}$FDR.

2.3. Identification of Candidate O-methyltransferases

We next sought to identify candidate OMTs potentially involved in flavonoid methylation. From the 16 differentially expressed putative methyltransferases identified in the transcriptomic analysis, candidates were assessed based on the presence of conserved Class II OMT motifs [9,29], methyltransferase-related gene annotations, and transcript abundance in leaves. Expression of eight putative OMTs were detected only in *E. eugenioides*, whereas the remaining eight were expressed in both species but differed in transcript abundance (Table S1). To prioritise candidates for functional testing, putative OMTs were ranked by transcript abundance in *E. eugenioides* leaves.

Five candidates were prioritised for experimental studies (Table S2). *EeOMT3* and *EeOMT4* were selected for further characterisation because they were among the most highly expressed candidates (Table S1). *EeOMT5* was included because of its high sequence similarity to *EeOMT3* and *EeOMT4*, sharing 96% and 94% pairwise identity, respectively (Figure 3). *EeOMT1* (the closest homolog of *EnOMT1*) was also included. In parallel, the predicted structure of *En*OMT1, a previously characterised 7-OMT in *E. nitida* [24], was used to identify additional candidates with structural similarity to known eucalypt OMTs. Alphafold-guided screening [30,31] identified 14 structurally similar proteins, with predicted local distance difference test (pLDDT) scores ranging from 79 to 94 (Table S3). One candidate, *EeOMT2*, showed a high pLDDT of 93 and its expression was detected in

 doi:10.20944/preprints202604.2208.v1

leaf RNA-seq data, so it was included for further characterisation. The nucleotide coding sequences and deduced amino acid sequences of the five candidates are shown in Table S2.

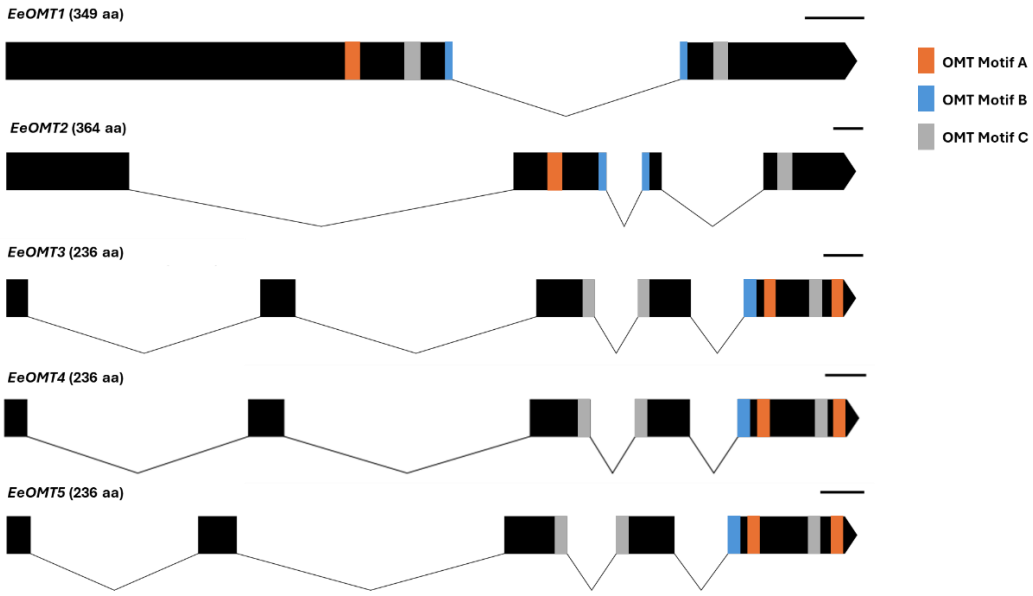

Figure 3. Gene structure of candidate *Eucalyptus* OMTs. Gene models were retrieved from the *E. grandis* reference genome (https://plants.ensembl.org/Eucalyptus_grandis/). Protein lengths are shown in brackets. Black boxes represent exons, and coloured boxes indicate conserved Class II OMT motifs: Motif A, (V/I/L)(V/L)(D/K)(V/I)GGXX(G/A); Motif B, (V/I/F)(A/P/E)X(A/P/G)DAXXXK(W/Y/F); and Motif C, (A/P/G/S)(L/I/V)(A/P/G/S)XX(A/P/G/S)(K/R)(V/I)(E/I)(L/I/V); Motif assignments allowed up to two amino acid mismatches [9,29]. Scale bar = 100 bp.

2.4. Flavonoid O-methyltransferase Activity of Candidate Genes

The five selected OMT candidates were cloned from *E. eugenioides* leaves and heterologously expressed in *E. coli* as recombinant proteins. Partially purified enzyme preparations were used to assess methylation activity against a panel of flavonoid substrates in the presence of *S*-adenosylmethionine, comprising the flavanones pinocembrin, naringenin, eriodictyol; the flavanonol taxifolin; the flavones chrysin, apigenin and luteolin; and the flavonol quercetin (Figure 4).

The recombinant OMTs exhibited distinct substrate preferences and methylation patterns. *Ee*OMT1 showed broad activity, catalysing *O*-methylation of all substrates tested (Figure 4A). Product profiles were dominated by 7-*O*-methylation, with minor amounts of di- and tri-methylated derivatives detected for eriodictyol, apigenin, luteolin and quercetin. These di- and tri-methylated derivatives retained 7-*O*-methylation with additional methylation(s) at the 3′ or 4′ positions of the B-ring, or at both positions.

*Ee*OMT2 methylated the 5-hydroxyl of pinocembrin to produce alpinetin, although conversion was low under the assay conditions used (4%). *Ee*OMT2 also methylated the equivalent 6′-hydroxyl of pinocembrin chalcone, with higher conversion observed for this substrate (27%). To assess whether *Ee*OMT2 could act on other A-ring-substituted flavanones, pinostrobin and cryptostrobin were tested as substrates. No methylation products corresponding to dimethylpinocembrin or 5-*O*-methylcryptostrobin were detected, suggesting that *Ee*OMT2 has narrow substrate specificity for A-ring methylation among the flavonoids tested. In addition to this observed A-ring/chalcone activity, *Ee*OMT2 methylated the 3′-hydroxyl of the B-ring of both flavanones and flavones in a strongly regioselective manner.

Liquid chromatography-mass spectrometry (LCMS) was used to characterise the product formed by *Ee*OMT2 from pinocembrin chalcone. The product showed an exact mass of *m/z* 271.0968 $[M+H]^+$, consistent with the molecular formula $C_{16}H_{14}O_4$ (calc. 271.0965). This is an increase of 14 mass

 doi:10.20944/preprints202604.2208.v1

units compared to pinocembrin chalcone (exact mass of *m*/*z* 257.0813 amu $[M+H]^+$) and is consistent with replacement of a hydroxyl proton with a methyl group to form an *O*-methylated product. The product exhibited a broad peak in the UV spectrum at 343 nm, which is characteristically associated with the B-ring cinnamoyl system in chalcones [32], and distinguished it from the methylated flavanones, alpinetin and pinostrobin, which have much narrower absorbances with λ_{max} of 285 and 289 nm, respectively. Methylation of pinocembrin chalcone by *Ee*OMT1 generated an isomeric product with the same exact mass but a later retention time and a slightly shifted UV λ_{max} at 339 nm. The *Ee*OMT2-derived methylated chalcone was chemically isomerised to alpinetin with acetic acid, and conversely, authentic alpinetin was chemically converted to a compound matching the *Ee*OMT2 product's retention time, UV spectrum and MS data. Together, the data support assignment of the *Ee*OMT2 product as alpinetin chalcone.

The other candidates, *Ee*OMT3-5, displayed narrower activity profiles. All three enzymes methylated substrates containing both 3′ and 4′-hydroxyl groups on the B-ring, but no detectable activity towards substrates containing only a 4′-hydroxyl group, such as naringenin and apigenin. *Ee*OMT3 exhibited highly specific activity towards the flavone luteolin and flavonol quercetin, with little detectable conversion of the flavanone eriodictyol or flavanonol taxifolin. It was the only enzyme in this study that methylated exclusively at one position, the 3′-hydroxyl of the B-ring. *Ee*OMT4 showed substrate preferences similar to *Ee*OMT3 but also produced di- and tri-methylated products, indicating capacity for sequential methylation at other sites (Figure 4B). *Ee*OMT5 showed the broadest activity, converting B-ring hydroxylated substrates including eriodictyol, luteolin, taxifolin and quercetin, into mixtures of mono-, di- and tri-methylated products. Notably, the tri-methylated products generated by *Ee*OMT4 and *Ee*OMT5 included methylation at the 3-hydroxyl of the flavonol C-ring of quercetin, but not at the equivalent position in the flavanonol taxifolin.

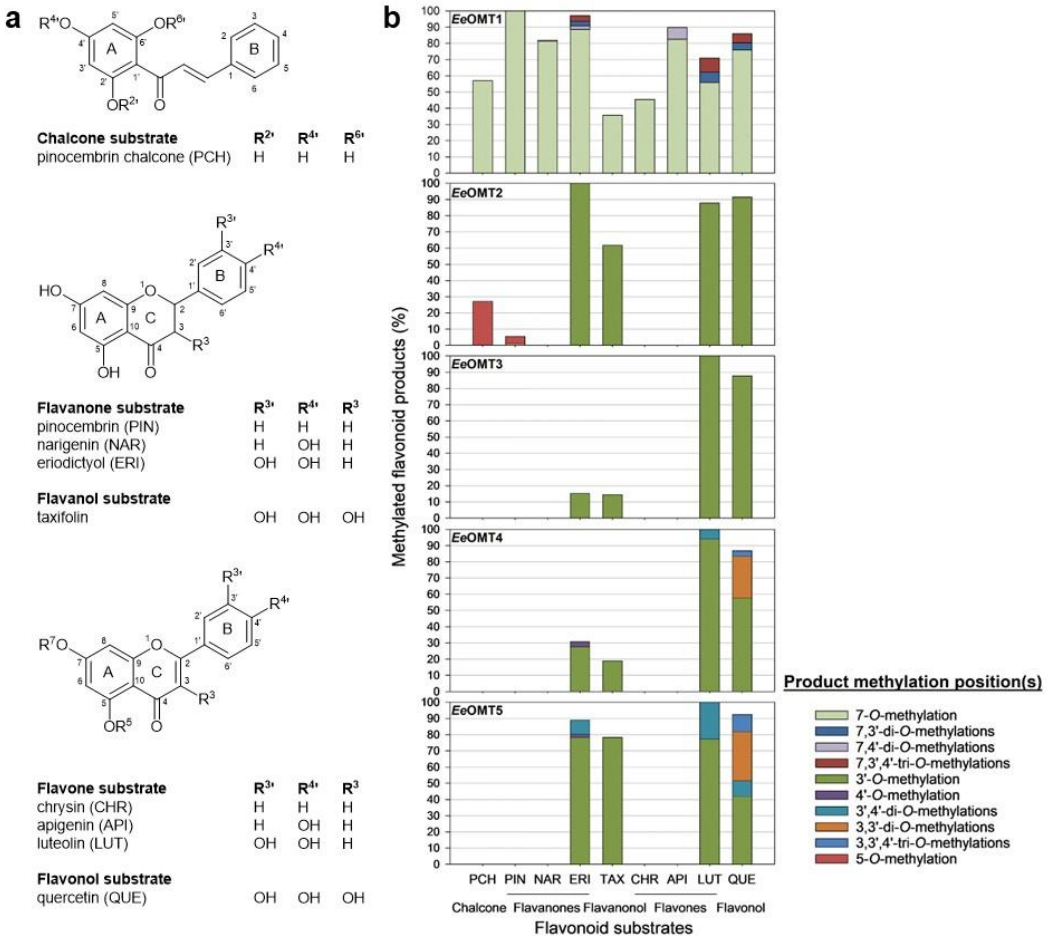

 doi:10.20944/preprints202604.2208.v1

Figure 4. Flavonoid *O*-methyltransferase activity and substrate preferences of candidate OMTs. (**a**) Chemical structures of the flavonoids tested as substrates. (**b**) Relative methylation activity of recombinant *E. eugenioides* toward the flavonoid substrates. Activities are expressed as percentages and were normalised separately for each enzyme to the substrate showing the highest activity: *Ee*OMT1, pinocembrin; *Ee*OMT2, eriodictyol; *Ee*OMT3-5, luteolin. All substrates were assayed with a substrate concentration of 100 µM in the presence of excess SAM (500 µM).

2.5. EeOMT2 Enzyme Kinetics and Substrate Specificity

To examine the activity of *Ee*OMT2 towards pinocembrin and pinocembrin chalcone, enzyme kinetic assays were performed using affinity-purified protein, an excess of SAM (500 µM), and varying substrate concentrations under assay conditions optimized for each substrate. For pinocembrin chalcone, *Ee*OMT2 showed an apparent K_M value of 6 µM, an apparent k_{cat} of 0.003 min^{-1} and k_{cat}/K_M of 5 x 10^{-4} μM^{-1} min^{-1}. By contrast, the activity for *Ee*OMT2 towards pinocembrin was barely detectable and accurate kinetic parameters could not be measured. Likewise, no activity could be detected for *Ee*OMT2 against pinostrobin chalcone or 2′,3′,4′-trihydroxychalcone, an isomer of pinocembrin chalcone with the 6′-hydroxyl moved to the 3′ position.

2.6. EeOMT1/EeOMT2 Expression and O-methylated Flavanone Accumulation

Variation in the accumulation of 5- and 7-*O*-methylated flavanones in leaves was observed across five *E. eugenioides* genotypes. We therefore examined whether transcript abundance of *EeOMT1* and *EeOMT2* was consistent with the accumulation patterns of their predicted flavanone products (Figure 5). Relative expression of *EeOMT2* in leaves broadly corresponded with the abundance of 5-*O*-methylated flavanones, comprising alpinetin and 5-*O*-methylcryptostrobin. Trees 1 and 2 showed significantly higher *EeOMT2* transcript abundance and accumulated higher levels of 5-*O*-methylated products than tree 5, which showed the lowest abundance of these metabolites (Figure 5A and C). In a similar way, increased *EeOMT1* expression was associated with the accumulation of 7-*O*-methylated flavanones. Tree 5, which accumulated the highest levels of 7-*O*-methylated compounds, showed the highest *EeOMT1* transcript abundance, whereas the remaining genotypes exhibited lower *EeOMT1* expression, and little to no accumulation of 7-*O*-methylated flavanones (Figure 5B and D). Together, these expression–metabolite patterns support the proposed roles of *Ee*OMT2 and *Ee*OMT1 in the formation of 5-*O*- and 7-*O*-methylated flavanones, respectively, in *E. eugenioides*.

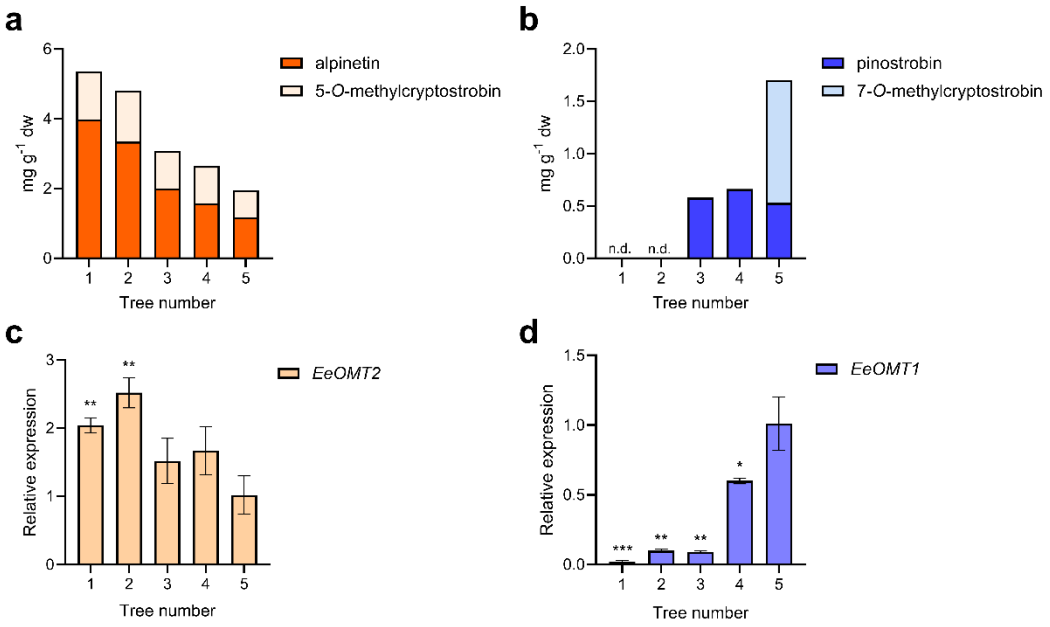

 doi:10.20944/preprints202604.2208.v1

Figure 5. Leaf flavanone profiles and relative expression of *EeOMT1* and *EeOMT2* in five *E. eugenioides* trees. (**a**) Total abundance of 5-*O*-methylated flavanones, comprising alpinetin (ALP) and 5-*O*-methylcryptostrobin (5-*O*-CS), in leaves of five representative *E. eugenioides* trees. (**b**) Total abundance of 7-*O*-methylated flavanones, comprising pinostrobin and 7-*O*-methylcryptostrobin. (**c**,**d**) Relative transcript abundance of *EeOMT1* and *EeOMT2* in leaves from the same trees. Metabolite abundances are expressed as mg g^{-1} of dry weight. Gene expression values are shown as mean ± SD from three independent replicates. Asterisks indicate statistically significant differences relative to tree 5, which was used as the calibrator: $p < 0.05$ (*) and $p < 0.01$ (**), using unpaired Student's *t*-tests.

3. Discussion

This study identifies a set of *Eucalyptus O*-methyltransferases with distinct activities toward flavonoid substrates and provides evidence for a chalcone-stage methylation for the 5-*O*-methylated flavanone alpinetin. Comparative transcriptomics of two eucalypt species with contrasting flavanone profiles, combined with conserved OMT motif analysis, protein-structure-guided candidate selection and recombinant enzyme assays, identified five candidate OMTs with divergent substrate preferences. Among these, *Ee*OMT2 was of particular interest because it methylated pinocembrin chalcone to form alpinetin chalcone, while showing relatively weak activity toward the corresponding flavanone, pinocembrin. These findings support a model in which 5-*O*-methylated flavanones in eucalypts arise through methylation of chalcone precursors before flavanone ring closure by an as-yet-unknown chalcone isomerase.

The activity of *Ee*OMT2 provides a plausible biochemical solution to the problem of flavanone 5-*O*-methylation. This enzyme also catalysed direct methylation of pinocembrin to alpinetin but activity was barely detectable under the assay conditions used, consistent with previous reports of low-yield alpinetin formation by bacterial OMTs [26]. In flavanones, the 5-hydroxyl group forms a strong intramolecular hydrogen bond with the adjacent 4-carbonyl, which reduces its accessibility and acidity relative to other phenolic hydroxyl groups [33]. Methylation at the chalcone stage may avoid this constraint because the corresponding 6′-hydroxyl of pinocembrin chalcone (which is the equivalent position to flavanone 5-hydroxyl) is more accessible for enzyme-catalysed deprotonation and methyl transfer. Consistent with this argument, *Ee*OMT2 methylated pinocembrin chalcone more efficiently than pinocembrin, and did not methylate 2′,3′,4′-trihydroxychalcone, which lacks the 6′-hydroxyl of pinocembrin chalcone.

The low activity of *Ee*OMT2 on pinocembrin to form alpinetin directly is reminiscent of a previous study which reported the activity of two Mg^{2+}-dependent bacterial OMTs (StrAOMT and DesAOMT) on pinocembrin to produce alpinetin with similar low efficiency [34]. Unlike *Ee*OMT2, however, these bacterial OMTs are Mg^{2+}–dependent, a metal cofactor that can coordinate the carbonyl oxygen and the 5-hydroxyl oxygen of the substrate to stabilize the reaction intermediate. The isolated *EeOMT2* sequence showed structural similarity to a plant flavanone CMT [27] and another eucalypt OMT, *EnOMT1* [24], which catalyses the 7-*O*-methylation. Both *Ee*OMT1 (encoded by the homolog of *EnOMT1*) and *Ee*OMT2 were shown here to act on pinocembrin chalcone, but *Ee*OMT1 showed a much greater efficiency towards pinocembrin. The opposite was observed for *Ee*OMT2 and in concert with transcriptomic evidence for its expression in leaves, is thus likely to be involved in alpinetin biosynthesis *in planta*. [34]. Based on *Ee*OMT2 catalytic activity, an alternative biosynthetic pathway for alpinetin is proposed (Figure 6).

The conversion of alpinetin chalcone to alpinetin remains unresolved. Both *At*CHI2 from *Arabidopsis thaliana* [35] and *Ee*CHI1 (Table S2) converted pinocembrin chalcone to pinocembrin and pinostrobin chalcone to pinostrobin, but neither enzyme converted alpinetin chalcone to alpinetin under the conditions tested. This suggests that alpinetin chalcone may require a distinct chalcone isomerase, an accessory factor, or favourable cellular conditions for efficient conversion in eucalypts.

Another OMT was identified, *Ee*OMT1, which showed broad 7-*O*-methyltransferase activity across nine substrates within the flavonoid panel (Figure 4), irrespective of other ring substitutions, consistent with the previously characterised *E. nitida* homolog *En*OMT1 [24]. In addition, *Ee*OMT1

 doi:10.20944/preprints202604.2208.v1

could 7-*O*-methylate alpinetin, alpinetin chalcone and the *C*-methylated flavanones purified from eucalypts. Dimethylpinocembrin may be biosynthesised by *Ee*OMT1 via the 7-*O*-methylation of alpinetin, a second methylation step with experimental precedent in the action of *En*OMT1 on alpinetin [24]. The biosynthesis of 5-*O*-methyl cryptostrobin is thought to be by 6′-*O*-methylation of cryptostrobin chalcone by *Ee*OMT2 with the chalcone product isomerised to produce 5-*O*-methyl cryptostrobin, however, this remains to be experimentally demonstrated. Together, the activities of *Ee*OMT1 and *Ee*OMT2 provide a framework for proposing alternative routes to 7-*O*- and 5-*O*-methylated flavanones in *E. eugenioides*. These activities are consistent with the observed expression–metabolite associations across *E. eugenioides* genotypes, in which *EeOMT2* transcript abundance corresponded broadly with 5-*O*-methylated flavanone accumulation, while *EeOMT1* expression was associated with 7-*O*-methylated products.

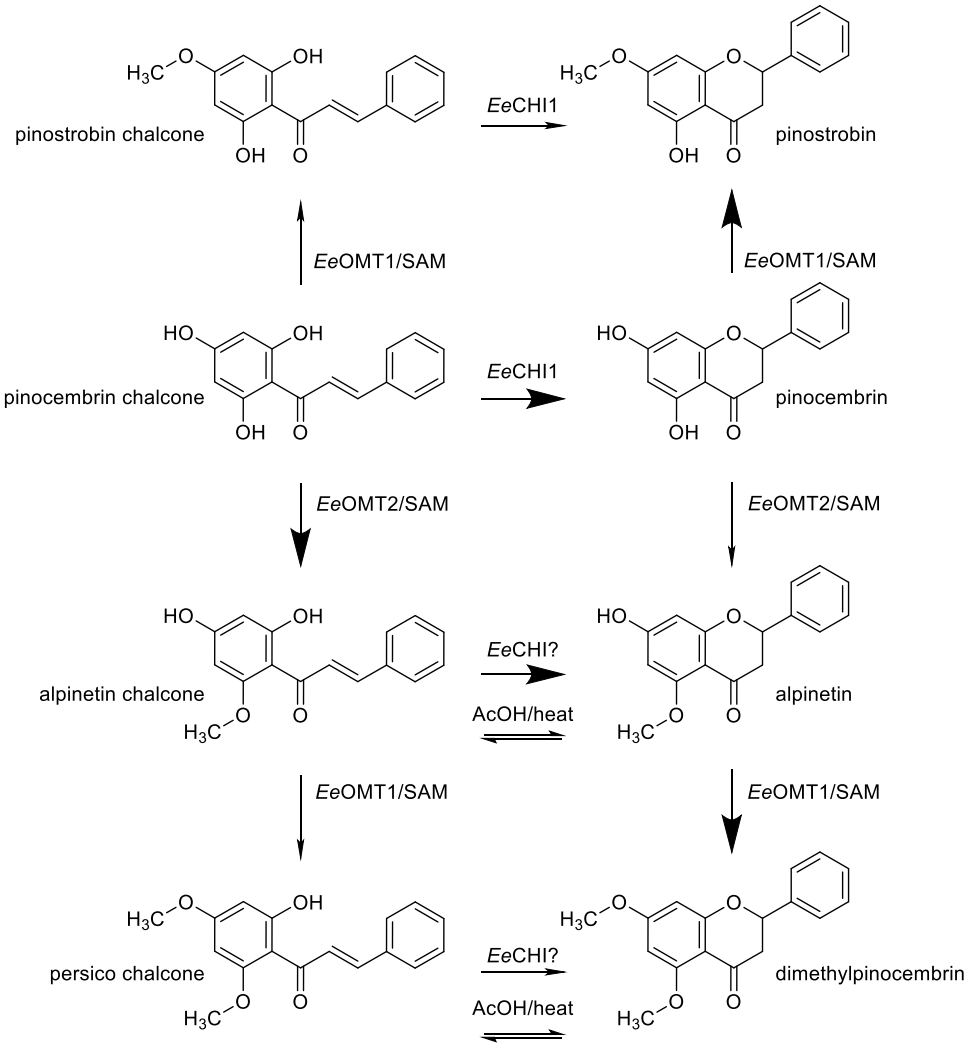

Figure 6. Summary of aspects of flavanone biosynthesis in eucalypts supported by this study. Larger arrows represent major pathways. Chemical isomerisation of alpinetin chalcone and persico chalcone by AcOH/heat are shown – this may require a distinct CHI *in planta* that has not yet been identified in eucalypts.

Moving beyond chalcone and A-ring methylation, *Ee*OMT2–*Ee*OMT5 possess the ability to catalyse flavonoid B-ring methylation. These enzymes methylated substrates that contain adjacent 3′- and 4′-hydroxyl groups, with a preference for 3′-*O*-methylation (Figure 4). *Ee*OMT2 was the most regioselective, producing only 3′-*O*-methylated products, whereas *Ee*OMT4 and *Ee*OMT5 produced additional di- and tri-methylated products, indicating capacity for sequential methylation of the flavonoid B-ring but favoring initial 3′-*O*-methylation. This preference for 3′-*O*-methylation is

 doi:10.20944/preprints202604.2208.v1

consistent with other plant flavonoid OMTs, including enzymes from *Glycine max* [36] and *Rhododendron delavayi* [27]. Unlike *Rd*OMT3, however, *Ee*OMT3 and *Ee*OMT5 retained activity toward substrates bearing a 4′-methoxy group, indicating differences in active-site tolerance among related flavonoid OMTs. The preference for methylation at the 3′-hydroxyl over the 4′-hydroxyl by *Ee*OMT3-5 was revealed by the low activity of the 3′-*O*-methylated flavonoids homoeriodictyol (3′-*O*-methyleriodictyol) and chrysoeriol (3′-*O*-methylluteolin). Conversely, *Ee*OMT3 and *Ee*OMT5 catalysed 3′-*O*-methylation of the 4′-*O*-methylated flavonoids hesperetin (4′-*O*-methyleriodictyol) and diosmetin (4′-*O*-methylluteolin) as substrates. All three enzymes were also incapable of methylating the 4′-hydroxyl in flavonoids possessing only a 4′-hydroxyl group on the B-ring (the flavanone naringenin and flavone apigenin), suggesting that these enzymes can be considered 3′-*O*-methylating OMTs.

Flavanones and flavones have different geometric structures with flavones being planar due to the double bond in the C-ring and flavanones being non-planar and chiral due to their stereogenic C2 [37]. *Ee*OMT3 and *Ee*OMT4 preferentially methylated the flavone luteolin over the identically substituted flavanone eriodictyol (Figure 4). This preference for the more planar flavones versus chiral flavanone matches the flavone substrate preference of four 3′-OMTs (*Gm*OMTs) identified in *G. max* [36]. On the other hand, *Ee*OMT5 showed weaker substrate preference for the flavone luteolin.

*Ee*OMT4 and *Ee*OMT5 also catalysed methylation at the 3-hydroxyl on the C-ring of the flavonol quercetin to a limited degree, but not the equivalent position in the flavanonol taxifolin. The observation of flavonol 3-*O*-methylation is noteworthy as methylation at this site is relatively uncommon in plants [38]. Unlike *Ee*OMT4 and *Ee*OMT5, most identified flavonoid 3-OMTs specifically methylate the 3-hydroxyl and are incapable of methylating hydroxyl groups on other rings. For example, an OMT from *R. delavayi* (*Rd*OMT10) was shown to methylate the flavonols, kaempferol, quercetin, and isorhamnetin regiospecifically to their 3-*O*-methylated products [27]. On the contrary, *Ee*OMT4 and *Ee*OMT5 showed sequential 3′/3-di-*O*-methylation activity on quercetin and thus appear to have a broader substrate site specificity.

*Ee*OMT3, *Ee*OMT4 and *Ee*OMT5 share 94–96% pairwise sequence identity, indicating that these functional differences arise from minor sequence variations. The high sequence similarity among these enzymes suggests that they are paralogs derived from gene duplication events, followed by subsequent neofunctionalization to enzymes that can generate a broad suite of methylated flavonoid secondary metabolites. Identifying the specific amino acid residues responsible for these functional differences will provide useful targets for engineering OMTs with tailored flavonoid methylation activities.

4. Materials and Methods

4.1. Plant Material

Newly developed, unexpanded leaves, approximately 2-3 weeks old were collected from selected *E. eugenioides* and *E. stenostoma* trees growing in a plantation in central Victoria, Australia (36.4641° S, 146.0213° E). For molecular analysis, up to 10 young leaves were immediately snap-frozen in liquid nitrogen and transported to the laboratory. For flavanone quantification and structural elucidation, bulk samples of fully expanded leaves, up to 100 leaves per tree, were collected from the same trees. Leaves were oven dried at 50 °C for 72 h and ground using a mill (MF10 microfine grinder drive; IKA-Werke, Breisgau, Germany) fitted with a cutting/grinding head and a 1 mm sieve.

4.2. RNA Isolation and Expression Analysis (qRT-PCR)

RNA was isolated from leaf tissue (300–400 mg) using a CTAB-based method [39], with the following modifications. After chloroform extraction, an equal volume of isopropanol was added to the aqueous phase and the mixture was incubated at room temperature for 10 min, followed by centrifugation at 15,000 × *g* for 20 min at 4 °C. The resulting pellet was washed with 600 µL of 70% (v/v) ethanol and resuspended in RNase-free water. RNA samples were further purified using the

 doi:10.20944/preprints202604.2208.v1

Spectrum Plant Total RNA Kit (Merck, Darmstadt, Germany) and treated with on-column DNase I, according to the manufacturer's instructions. Approximately 1.5 µg of total RNA was used for first-strand cDNA synthesis with the Tetro cDNA Synthesis Kit (Bioline, London, UK), in a total reaction volume of 20 µL. Reactions were incubated at 45 °C for 30 min and were terminated by heating at 85 °C for 5 min. The resulting cDNA was diluted 1:16 for subsequent analysis. qRT-PCR analysis was performed using SYBR Green (Thermo Fisher Scientific) according to the manufacturer's instructions on a CFX384 Touch Real-Time PCR detection system (Bio-Rad Laboratories, Hercules, USA). Oligonucleotide sequences are listed in Table S5. Cycling conditions were 95 °C for 2 min, followed by 30 cycles of 95 °C for 5 s and 60 °C for 10 s. Melt curve analysis was performed using the real-time cycler's built-in program. Relative expression levels were calculated using the $2^{-\Delta\Delta CT}$ method [40], with *α-tubulin* as the housekeeping gene and *E. eugenioides* tree #5 as calibrator, set to a relative expression value of 1.

4.3. Transcriptome Sequencing

Total RNA samples from unexpanded leaves were prepared using the Illumina's TruSeq Stranded RNA library preparation and sequenced at the Australian Genome Research Facility (AGRF; Melbourne, Australia) on an Illumina NovaSeq X Plus RNA-seq platform, generating 150 bp paired-end reads. Raw reads were quality-checked and filtered to remove Illumina adapter sequences, overrepresented sequences, and potential cross-species contamination. Across all samples, >91% of bases had a Phred quality score ≥ Q30. Filtered reads were aligned to the *E. grandis* reference genome (GCA_000612305.1) using STAR (v2.3.5a). Read mapping rates and distribution across genomic features were summarized (Table S4). Transcript assembly was performed using StringTie version 2.1.4 [41] with the reference annotation-based transcript (RABT) option, utilizing the RefSeq genome annotation as a guide. Differential expression analysis was conducted with edgeR version 4.0.9 in R [42]. Counts were normalized using the trimmed mean of M-values (TMM) method, and differential expression between groups was assessed using a generalized linear model (GLM) framework.

4.4. Cloning of Candidate OMTs

Full-length coding sequences of candidate OMTs (GenBank accession numbers: EeOMT1_CDS PZ332309; EeOMT2_CDS PZ332310; EeOMT3_CDS PZ332311; EeOMT4_CDS PZ332312; EeOMT5_CDS PZ332313; EeCHI1_CDS PZ332314) were amplified from *E. eugenioides* cDNA using 1.25 µL each of forward and reverse primers (10 mM; Table S5), 5 µL of 5x Phusion HF Buffer, 0.2 µL of Phusion HF polymerase (Thermo Fisher Scientific), 0.5 µL of 10 mM dNTPs and 16.3 µL of nuclease-free water in a total reaction volume of 25 µL. PCR was performed under the following reaction conditions: 98 °C for 30 s, 35 cycles of 98 °C for 10 s, 55 °C for 30 s and 72 °C for 30 s kb^{-1}, followed by a final extension 72 °C for 5 min and 4 °C hold. Purified PCR products were digested with the appropriate restriction enzymes (*BamHI*, *EcoRI*, or *NotI*) and the pHUE vector, which contains an N-terminal 6×His tag and a thrombin cleavage site, was linearised using the same enzymes with the addition of 1 µL TSAP (Promega, Madison, USA). Following gel purification, T4 DNA ligations were set up for each candidate OMT according to the manufacturer's instructions (Thermo Fisher Scientific, Waltham, USA), and 5 µL of each ligation reaction was transformed into *E. coli* DH5α cells. Plasmids were purified using the ZR Plasmid Miniprep Classic kit (Zymo Research, Irvine, USA) and verified by Sanger sequencing at AGRF. Sequence-verified plasmids were subsequently transformed into *E. coli* BL21 (DE3) cells for enzyme assays.

4.5. Recombinant Protein Expression

Cells of *E. coli* BL21 (DE3) harbouring the expression vectors were grown in 100 mL LB medium supplemented with carbenicillin (100 µg mL^{-1}) at 37 °C for approximately 5 h, until the culture reached an OD 600 of 0.6. Protein production was induced by the addition of 0.1 mM isopropyl β-D-

 doi:10.20944/preprints202604.2208.v1

1-thiogalactopyranoside and cultures were incubated at 16 °C for 16 h [24]. Cells were harvested by centrifugation (3,000 × *g* for 5 min) and the pellet was resuspended in lysis buffer (50 mM NaH_2PO_4, 300 mM NaCl, 10 mM imidazole), supplemented with protease inhibitor cocktail (Roche, Basel, Switzerland) and 1 mg mL^{-1} Lysozyme (Thermo Fisher Scientific). The suspension was gently mixed at room temperature for 30 min and sonicated to release intracellular content. The lysate was centrifuged twice at 10,000 × *g* for 5 min, and the clarified supernatant was used as crude enzyme extract for the enzyme assays.

4.6. Enzyme Assays and Kinetics

Enzyme activity of crude extracts was assayed as described [24], with the following modifications: reaction mixtures contained 50 mM sodium phosphate buffer (pH 7), 200 µL of crude OMT enzyme (approx. 0.6 mg of total protein), 500 µM S-adenosyl-L-methionine (SAM), and 100 µM substrate dissolved in DMSO, in a total reaction volume of 500 µL. Reactions were incubated at 30 °C with gentle shaking for 2 h and terminated by the addition of an equal volume of acetonitrile. The solvent fraction of the assay mixture containing methylated products was separated overnight at -20 °C and subsequently analysed by HPLC. Negative controls (reactions lacking enzyme, substrate or SAM) were included alongside experimental samples to ensure analytical accuracy. All authentic flavonoid standards used as substrates and to identify methylated products were purchased from Extrasynthese (Genay, France).

*Ee*OMT2 was purified with immobilized metal affinity chromatography and quantified with bicinchoninic acid (BCA) assay for enzyme kinetic assays. Enzyme kinetic parameters of *Ee*OMT2 were calculated using pinocembrin chalcone and pinocembrin as substrates. The enzyme kinetics assays were performed with the same procedure mentioned above with the following modifications: reaction mixtures contained 50 mM sodium phosphate buffer (pH 7 for pinocembrin assays and pH 5.5 for pinocembrin chalcone assays), 30 µL of purified EeOMT2 enzyme (72 µg of total protein), and 30 µL of SAM (10 mM) in a total reaction volume of 750 µL at 15 °C. Duplicate assays with the purified enzyme and varying substrate concentrations (2–100 µM) at a final concentration of 400 µM SAM were carried out for time intervals ranging from 30 to 80 min, where the reaction velocity is in the linear range with respect to time for *Ee*OMT2 with pinocembrin chalcone and pinocembrin as substrates. The kinetic constants (V_{max} and K_M) were determined using the Enzyme Kinetics add-on in SigmaPlot version 16 (Grafiti LLC, Palo Alto, USA). The catalytic rate constant (k_{cat}) was calculated from V_{max} using the concentration of purified *Ee*OMT2.

4.7. Chemical and Enzymic Rearrangement of Chalcones to Flavanones

Alpinetin chalcone, the methylated product produced by *Ee*OMT2 on pinocembrin chalcone, was subjected to chemical isomerisation to alpinetin. The product mixture was dried and reconstituted in glacial acetic acid (300 µL). The solution was then heated at 70 °C for 16 h. Following incubation, the mixture was dried and redissolved in acetonitrile (300 µL) prior to HPLC analysis. The same protocol was also applied to rearrange an authentic standard of alpinetin into alpinetin chalcone.

The coding sequence of a chalcone isomerase (chalcone-flavanone isomerase; *AtCHI2*; UniProt: Q9FKW3) from *Arabidopsis thaliana* was *de novo* synthesised as a gene block (Twist Bioscience, San Francisco, USA) to assess its activity toward the flavanone chalcone substrates pinocembrin chalcone, pinostrobin chalcone and alpinetin chalcone. The *AtCHI2* CDS sequence included restriction site overhangs (*BamHI* and *NotI*) enabling cloning into the pHUE expression vector. The candidate *EeCHI1*, identified through AlphaFold-guided homology searches using the *At*CHI2 protein sequence as a query, was selected based on its expression in leaves and subsequently isolated and cloned from *E. eugenioides* cDNA using the primers described in Table S5. Recombinant protein expression was carried out as described in section 4.5, with the modification of reducing temperature to 15 °C to minimise possible spontaneous rearrangement of chalcones to their respective flavanones [43].

 doi:10.20944/preprints202604.2208.v1

4.8. HPLC and LCMS

HPLC was performed using a Prominence system (Shimadzu Corporation, Kyoto, Japan) fitted with a Phenomenex Gemini C18 column (Danaher, Washington, USA) eluted at a flow rate of 1.0 mL min^{-1} [19]. LCMS analysis was performed using an Agilent Revident 6520 accurate-mass QTOF mass spectrometry system (Agilent Technologies, Santa Clara, USA), with a dual electro-spray ionisation source attached to an Agilent 1200 Infinity HPLC with a diode array detector using the same column and eluent system as the HPLC, but with a flow rate of 0.8 mL min^{-1}. The LCMS was run in both positive and negative modes with an ion-source voltage of 150V (CID of 10).

Flavonoids in leaf extracts and bioassays were identified and quantified based on comparison to authentic standards (Extrasynthese) or compounds purified in-house and using the characteristic LCMS fragmentation patterns of flavonoids [44,45]. In addition, the identities of 7-*O*-methylcryptostrobin, 7-*O*-methyldemethoxymatteucinol and 5,7-di-*O*-methylcryptostrobin were confirmed by the action of the recombinant protein of *En*OMT1 on cryptostrobin, demethoxymatteucinol and 5-*O*-methylcryptostrobin substrates, respectively.

4.9. Nuclear Magnetic Resonance (NMR) Spectroscopy

NMR spectra were collected on a Bruker Avance spectrometer (Bruker Corporation, Billerica, USA), ^{1}H NMR 500 MHz and ^{13}C NMR 125 MHz. Compound 1 was dissolved in methanol-d_4 (MeOD), and compound 2 was dissolved in chloroform-d_1 ($CDCl_3$). Spectra were referenced to the residual solvent peaks (MeOD: δ 3.31 ppm and δ 49.00 ppm; $CDCl_3$: δ 7.26 ppm and δ 77.16 ppm). Chemical shifts (δ) are reported in parts per million (ppm) and coupling constants (J) are reported in Hz. Multiplicities are reported as follows: s, singlet; d, doublet; dd, doublet of doublets; t, triplet; sept, septet; m, multiplet (Appendix A1).

4.10. X-Ray Diffraction

X-ray diffraction data (Appendix A1) were collected on a Rigaku Synergy S X-ray diffractometer equipped with a Cu Kα sealed X-ray tube. Cell refinement and data reduction were performed in CrysAlisPro [46]. Structures were refined in WinGX [47] using the SHELX suite [48].

5. Conclusions

The functional characterisation of eucalypt OMTs revealed a chalcone OMT (*Ee*OMT2) that can produce alpinetin chalcone, a plausible direct biosynthetic precursor of alpinetin. We propose a novel biosynthetic pathway of 5-*O*-methylated flavanones directly from their respective chalcones, rather than via flavanones. Understanding the biosynthesis of alpinetin and related compounds can guide efforts to enhance beneficial flavanones in functional foods or produce high-value metabolites via synthetic biology. Other candidate OMTs also exhibited promising activities regarding the methylation of flavonoids. Broad-spectrum enzymes such as *Ee*OMT1 could enable the production of diverse methylated flavonoids in heterologous systems, while highly selective enzymes (*Ee*OMT2–5) offer precise control over flavonoid scaffold modification, particularly with respect to B- and C-ring methylation and the relative preference for flavanones or flavones. Complementary downstream assays are key to determining how these methylation patterns influence pharmacological and therapeutic properties. Future work may focus on heterologous pathway reconstruction of flavonoid biosynthesis, structural validation of OMT/substrate interactions, and *in planta* functional analysis through transient expression or knockouts approaches.

Supplementary Materials: The following supporting information can be downloaded at: https://www.mdpi.com/article/doi/s1, Figure S1: ORTEP representation of the asymmetric unit of compound 1 (5-*O*-methylcryptostrobin), as determined by X-ray diffraction; Table S1: Putative methyltransferases identified from differential gene expression analyses between *E. eugenioides* and *E. stenostoma*; Table S2: Nucleotide (CDS) and deduced amino acid sequences of candidate OMTs and isomerase identified and cloned from *E. eugenioides*

 doi:10.20944/preprints202604.2208.v1

leaves; Table S3: Summary of predicted proteins structurally similar to EnOMT1 identified using AlphaFold Database; Table S4: Summary of RNA-seq read mapping and feature assignment statistics; Table S5: List of oligos used for cloning and qRT-PCR; Table S6: Comparison of literature NMR data with the observed experimental NMR data.

Author Contributions: Conceptualization, L.Z., G.G.G., J.H. and J.Q.D.G.; methodology, L.Z., G.G.G., J.H. and A.S.; formal analysis, L.Z., G.G.G., J.H., A.S. and J.Q.D.G.; investigation, L.Z., G.G.G., J.H. and A.S.; resources, S.J.W. and J.Q.D.G.; writing—original draft preparation, L.Z., G.G.G. and A.S.; writing—review and editing, J.H., S.J.W. and J.Q.D.G.; supervision, G.G.G, S.J.W. and J.Q.D.G.; funding acquisition, J.Q.D.G. and S.J.W. All authors have read and agreed to the published version of the manuscript.

Funding: This research was funded by Australian Research Council, grant numbers IM240100129, DP240100126, and DP250100819.

Institutional Review Board Statement: Not applicable.

Informed Consent Statement: Not applicable.

Data Availability Statement: Sequence data have been submitted to GenBank and are available from the corresponding author upon reasonable request pending public release. CCDC 2453271 contains the X-ray diffraction crystallographic data for this paper. This data can be obtained free of charge via www.ccdc.cam.ac.uk/data_request/cif, or by emailing data_request@ccdc.cam.ac.uk, or by contacting the Cambridge Crystallographic Data Centre, 12 Union Road, Cambridge CB2 1EZ, UK; fax: +44 1223 336033.

Acknowledgments: The authors thank Gretals Australia Ltd. for support and access to the plantation, and acknowledge the Magnetic Resonance and Proteomics platforms at the University of Melbourne, and the Australian Synchrotron (Australian Nuclear Science and Technology Organisation).

Conflicts of Interest: The authors declare no conflicts of interest. The funders had no role in the design of the study; in the collection, analyses, or interpretation of data; in the writing of the manuscript; or in the decision to publish the results.

Abbreviations

The following abbreviations are used in this manuscript:

CMT	*C*-methyltransferase
DEGs	Differentially expressed genes
FDR	False discovery rate
FE	Fold enrichment
HPLC	High performance liquid chromatography
KEGG	Kyoto encyclopedia of genes and genomes
LCMS	Liquid chromatography-mass spectrometry
NMR	Nuclear magnetic resonance spectroscopy
OMT	*O*-methyltransferase
PCR	Polymerase chain reaction
pLDDT	Predicted local distance difference test
qRT-PCR	Quantitative reverse transcription PCR
SAM	S-adenosyl-L-methionine

Appendix A

Appendix A.1 Structural Elucidation of C-methylated Flavanones

Two putative flavanones in the eucalypt leaf extracts could not be definitively identified by comparison to available commercial or in-house flavanone standards. Their MS data was identical, with an exact mass of *m/z* 285.1103 $[M+H]^+$, corresponding to the molecular formula $C_{17}H_{16}O_4$ (calcd for $[M+H]^+$, 285.1127), consistent with dimethylated flavanones. To identify the compounds, bulk

 doi:10.20944/preprints202604.2208.v1

acetonitrile extraction of *E. eugenioides* leaves (100 g) was performed, and the extract was fractionated using a Reveleris X2 medium-pressure liquid chromatography system fitted with a Büchi FlashPure Select C-18 cartridge (4 g; Büchi Labortechnik, Flawil, Switzerland), using the same mobile phases as for HPLC. Both compounds were obtained as white crystals.

The ^{1}H NMR spectrum of compound 1 showed two methyl singlets at δ 2.01 ppm (3H, s, *C*-Me) and 3.80 ppm (3H, s, *O*-Me), indicating the presence of *C*-methyl and *O*-methyl groups (Table S6). Four possible isomers are consistent with this methylation pattern, and the NMR spectra alone did not allow unambiguous assignment. Compound 1 was therefore crystallized, and its structure was determined by single-crystal X-ray diffraction. Crystals were grown by slow diffusion of n-hexane into ethyl acetate, and intensity data were collected on a Rigaku Synergy S diffractometer (Rigaku Corporation, Tokyo, Japan) using Cu Kα radiation. Crystal data: $C_{17}H_{16}O_4$, Mr = 284.30, T = 100 K, λ = 1.54184 Å, monoclinic, space group C2, a = 23.0977(5) Å, b = 5.12320(10) Å, c = 24.3060(5) Å, α = 90°, β = 99.940(2)°, γ = 90°, V = 2833.05(10) Å^3, Z = 8, Dc = 1.333 g cm^{-3}, μ 0.778 mm^{-1} (Cu), F(000) = 1200, crystal size = 0.101 × 0.050 × 0.034 mm^3. A total of 16,601 reflections were measured to θmax = 79.134°, yielding 5,920 independent reflections [R(int) = 0.0764]. Final refinement gave R = 0.0502 and wR(F2) = 0.1207 [I > 2σ(I)], with goodness of fit = 1.071. The absolute structure parameter was 0.06(17). CCDC: 2453271. X-ray diffraction established the structure of compound 1 as 5-*O*-methyl cryptostrobin with an (*S*) configuration (Figure S1). The NMR data for compound 1 were in good agreement with a previous report of this compound [49].

The ^{1}H NMR spectrum of compound 2 showed two methyl singlet signals at δ 2.01 ppm (3H, s, H-11) and 3.84 ppm (3H, s, H-12), consistent with a *C*-methyl group and an *O*-methyl group (Table S6). The HMBC spectrum showed correlations from both methyl signals to the same carbon signal at δ_C 165.77 ppm (C-7), indicating that the methyl and methoxy groups are ortho to each other. In addition, the *C*-methyl singlet signal at δ_H 2.01 ppm and the H-2 signal at 5.42 ppm showed HMBC correlations to the same carbon signal at δ_C 161.16 ppm (C-9), consistent with the attachment of the *C*-methyl group to C-8. This assignment places the methoxy group at C-7. Compound 2 was therefore assigned as 7-*O*-methyl cryptostrobin, and its NMR data were in good agreement with the literature [50].

References

1. Ferreyra, M. L. F.; Serra, P.; Casati, P., Recent advances on the roles of flavonoids as plant protective molecules after UV and high light exposure. *Physiologia Plantarum* **2021,** 173, 736-749.
2. Jieting, W.; Sidi, L.; Lei, Z.; Tian, G.; Chang, Y.; Jianing, H.; Fang, M., Advances in the study of the function and mechanism of the action of flavonoids in plants under environmental stresses. *Planta* **2023,** 257.
3. Marie Louisa, R.; Claude, K.; Jean Jacques, H.; Valérie Le, C.; Latifa, H.; Emmanuel, G.; Mathilde, B., Role of phenylpropanoids and flavonoids in plant resistance to pests and diseases. *Molecules* **2022,** 27.
4. Bo, Y.; Jin, Z.; Mengxuan, Z.; Zongwu, L.; Liqun, R.; Fan, Z.; Cuizhe, L.; Lin, Z., Flavonoids: a natural remedy in the prevention and management of diverse diseases. *Frontiers in Medicine* **2025,** 12.
5. Duarte, M.; Pedrosa, S. S.; Khusial, P. R.; Madureira, A. R., The biological potential and health-benefits of flavonoids: A review and development opportunities. *Chemico-Biological Interactions* **2025,** 421, 111755.
6. Jincan, L.; Jinhai, L.; Zhili, S.; Zhonghao, F.; Yu, F.; Nannan, W.; Bao, Y.; Baojun, X., Latest research progress on anti-microbial effects, mechanisms of action, and product developments of dietary flavonoids: A systematic literature review. *Trends in Food Science and Technology* **2025,** 156.
7. Mehak, Z.; Heidi, A.; Blassan, P. G., Flavonoids: Antioxidant Powerhouses and Their Role in Nanomedicine. *Antioxidants* **2024,** 13.
8. Saleh, A.; Leonardo Perez de, S.; Maria, B.; Alisdair, R. F., The style and substance of plant flavonoid decoration; towards defining both structure and function. *Phytochemistry* **2020,** 174.
9. Chandrashekhar, P. J.; Vincent, L. C., Conserved sequence motifs in plant S-adenosyl-L-methionine-dependent methyltransferases. *Plant Molecular Biology* **1998,** 37, 663.
10. Yuting, L.; Alisdair, R. F.; Takayuki, T., Diversification of chemical structures of methoxylated flavonoids and genes encoding flavonoid-*O*-methyltransferases. *Plants* **2022,** 11.

 doi:10.20944/preprints202604.2208.v1

11. Thomas, W., Methylation of dietary flavones increases their metabolic stability and chemopreventive effects. *International Journal of Molecular Sciences* **2009,** 10, 5002-5019.
12. Aleksandra, W.; Paulina, S.-D.; Hanna, P.; Agnieszka, K.-Ł.; Karolina, S.; Tomasz, J.; Edyta, K.-S., Interaction of 4′-methylflavonoids with biological membranes, liposomes, and human albumin. *Scientific Reports* **2021,** 11.
13. Nicolle, D., Classification of the eucalypts, genus *Eucalyptus.* Version 7.1. In 2024.
14. Goodger, J. Q. D.; Senaratne, S. L.; Nicolle, D.; Woodrow, I. E., Foliar essential oil glands of *Eucalyptus* subgenus *Eucalyptus* (Myrtaceae) are a rich source of flavonoids and related non-volatile constituents. *PLoS ONE* **2016,** 11, e0151432.
15. Goodger, J. Q. D.; Senaratne, S. L.; van der Peet, P.; Browning, R.; Williams, S. J.; Nicolle, D.; Woodrow, I. E., *Eucalyptus* subgenus *Eucalyptus* (Myrtaceae) trees are abundant sources of medicinal pinocembrin and related methylated flavanones. *Industrial Crops and Products* **2019,** 131, 166-172.
16. Marsh, K. J.; Saraf, I.; Hocart, C. H.; Youngentob, K.; Singh, I.-P.; Foley, W. J., Occurrence and distribution of unsubstituted B-ring flavanones in *Eucalyptus* foliage. *Phytochemistry* **2019,** 160, 31-39.
17. Saraf, I.; Marsh, K.; Vir, S.; Foley, W.; Singh, I. P., Quantitative analysis of various B-ring unsubstituted and substituted flavonoids in ten Australian species of *Eucalyptus*. *Natural Product Communications* **2017,** 12, 1695-1699.
18. Courtney, J. L.; Lassak, E. V.; Speirs, G. B., Leaf wax constituents of some myrtaceous species. *Phytochemistry* **1983,** 22, (4), 947-949.
19. Heskes, A. M.; Goodger, J. Q. D.; Tsegay, S.; Quach, T.; Williams, S. J.; Woodrow, I. E., Localization of oleuropeyl glucose esters and a flavanone to secretory cavities of Myrtaceae. *PLOS One* **2012,** 7, (7), e40856.
20. Sabrina, C.; Gudrun, S.; Elke, W.; Dieter, S.; Jurgen, S.; Joachim, S., A flavonol *O*-methyltransferase from *Catharanthus roseus* performing two sequential methylations. *Phytochemistry* **2003**, 127-137.
21. Xiaojuan, L.; Yue, W.; Yezhi, C.; Shuting, X.; Qin, G.; Chenning, Z.; Jinping, C.; Chongde, S., Characterization of a flavonoid 3′/5′/7-*O*-methyltransferase from *Citrus reticulata* and evaluation of the in vitro cytotoxicity of its methylated products. *Molecules* **2020,** 25.
22. Man, Z.; Tao, W.; Qiaosheng, G.; Yong, S.; Feng, Y., Systematic identification and characterization of *O*-methyltransferase gene family members involved in flavonoid biosynthesis in *Chrysanthemum indicum* L. *International Journal of Molecular Sciences* **2024,** 25.
23. Jian Min, Z.; Yong Weon, S.; Ragai, K. I., Biochemical characterization of a putative wheat caffeic acid *O*-methyltransferase. *Plant Physiology and Biochemistry* **2009,** 47, 322-326 , pmid = 19211254.
24. Somaletha Chandran, K.; Humphries, J.; Goodger, J. Q. D.; Woodrow, I. E., Molecular characterisation of flavanone *O*-methylation in *Eucalyptus*. *International Journal of Molecular Sciences* **2022,** 23, (6), 3190.
25. Zhao, G.; Tong, Y.; Luan, F.; Zhu, W.; Zhan, C.; Qin, T.; An, W.; Zeng, N., Alpinetin: A Review of Its Pharmacology and Pharmacokinetics. *Front Pharmacol* **2022,** 13, 814370.
26. Peng, B.; Wang, Z.; Zhang, L.; Groves, M. R.; Haslinger, K., *De novo* biosynthesis of alpinetin enhanced by directed evolution of 5-*O*-methyltransferase. *Microbial Cell Factories* **2026**.
27. Zhang, M.; Bao, Y.-o.; Dai, Z.; Qian, Z.; Yu, H.; Zhou, J.-j.; Chen, Y.; Wang, Z.; Wang, K.; Cai, M.; Ye, M., Molecular and structural characterization of a chalcone di-*C*-methyltransferase RdCMT from *Rhododendron dauricum* and its application in *de novo* biosynthesis of farrerol in *Pichia pastoris*. *Journal of the American Chemical Society* **2025,** 147, (20), 17132-17143.
28. Myburg, A. A.; Grattapaglia, D.; Tuskan, G. A.; Hellsten, U.; Hayes, R. D.; Grimwood, J.; Jenkins, J.; Lindquist, E.; Tice, H.; Bauer, D.; Goodstein, D. M.; Dubchak, I.; Poliakov, A.; Mizrachi, E.; Kullan, A. R.; Hussey, S. G.; Pinard, D.; van der Merwe, K.; Singh, P.; van Jaarsveld, I.; Silva-Junior, O. B.; Togawa, R. C.; Pappas, M. R.; Faria, D. A.; Sansaloni, C. P.; Petroli, C. D.; Yang, X.; Ranjan, P.; Tschaplinski, T. J.; Ye, C. Y.; Li, T.; Sterck, L.; Vanneste, K.; Murat, F.; Soler, M.; Clemente, H. S.; Saidi, N.; Cassan-Wang, H.; Dunand, C.; Hefer, C. A.; Bornberg-Bauer, E.; Kersting, A. R.; Vining, K.; Amarasinghe, V.; Ranik, M.; Naithani, S.; Elser, J.; Boyd, A. E.; Liston, A.; Spatafora, J. W.; Dharmwardhana, P.; Raja, R.; Sullivan, C.; Romanel, E.; Alves-Ferreira, M.; Külheim, C.; Foley, W.; Carocha, V.; Paiva, J.; Kudrna, D.; Brommonschenkel, S. H.; Pasquali, G.; Byrne, M.; Rigault, P.; Tibbits, J.; Spokevicius, A.; Jones, R. C.; Steane, D. A.; Vaillancourt, R. E.; Potts, B. M.; Joubert, F.; Barry, K.; Pappas, G. J.; Strauss, S. H.; Jaiswal, P.; Grima-Pettenati, J.; Salse, J.;

 doi:10.20944/preprints202604.2208.v1

Van de Peer, Y.; Rokhsar, D. S.; Schmutz, J., The genome of *Eucalyptus grandis*. *Nature* **2014,** 510, (7505), 356-62.

29. Barakat, A.; Choi, A.; Yassin, N. B. M.; Park, J. S.; Sun, Z.; Carlson, J. E., Comparative genomics and evolutionary analyses of the *O*-methyltransferase gene family in *Populus*. *Gene* **2011,** 479, (1-2), 37-46.
30. Jumper, J.; Evans, R.; Pritzel, A.; Green, T.; Figurnov, M.; Ronneberger, O.; Tunyasuvunakool, K.; Bates, R.; Žídek, A.; Potapenko, A.; Bridgland, A.; Meyer, C.; Kohl, S. A. A.; Ballard, A. J.; Cowie, A.; Romera-Paredes, B.; Nikolov, S.; Jain, R.; Adler, J.; Back, T.; Petersen, S.; Reiman, D.; Clancy, E.; Zielinski, M.; Steinegger, M.; Pacholska, M.; Berghammer, T.; Bodenstein, S.; Silver, D.; Vinyals, O.; Senior, A. W.; Kavukcuoglu, K.; Kohli, P.; Hassabis, D., Highly accurate protein structure prediction with AlphaFold. *Nature* **2021,** 596, (7873), 583-589.
31. Varadi, M.; Anyango, S.; Deshpande, M.; Nair, S.; Natassia, C.; Yordanova, G.; Yuan, D.; Stroe, O.; Wood, G.; Laydon, A.; Žídek, A.; Green, T.; Tunyasuvunakool, K.; Petersen, S.; Jumper, J.; Clancy, E.; Green, R.; Vora, A.; Lutfi, M.; Figurnov, M.; Cowie, A.; Hobbs, N.; Kohli, P.; Kleywegt, G.; Birney, E.; Hassabis, D.; Velankar, S., AlphaFold Protein Structure Database: massively expanding the structural coverage of protein-sequence space with high-accuracy models. *Nucleic Acids Research* **2022,** 50, (D1), D439-D444.
32. Blanco, S. E.; Ferretti, F. H., Determination of absorptivity and formation constant of a chalcone association complex. *Talanta* **1998,** 45, (6), 1103-1109.
33. Musialik, M.; Kuzmicz, R.; Pawłowski, T. S.; Litwinienko, G., Acidity of hydroxyl groups: an overlooked influence on antiradical properties of flavonoids. *The Journal of Organic Chemistry* **2009,** 74, (7), 2699-2709.
34. Sokolova, N.; Zhang, L.; Deravi, S.; Oerlemans, R.; Groves, M. R.; Haslinger, K., Structural characterization and extended substrate scope analysis of two $Mg^{(2+)}$-dependent *O*-methyltransferases from Bacteria. *Chembiochem* **2023,** 24, (9), e202300076.
35. Hanko, E. K. R.; Robinson, C. J.; Bhanot, S.; Jervis, A. J.; Scrutton, N. S., Engineering an *Escherichia coli* strain for enhanced production of flavonoids derived from pinocembrin. *Microbial Cell Factories* **2024,** 23, (1), 312.
36. Feng, B.; Jiang, Y.; Li, X.; Wang, Y.; Ren, Z.; Lu, J.; Yan, X.; Zhou, Z.; Wang, P., Systemically functional characterization of regiospecific flavonoid *O*-methyltransferases from *Glycine max*. *Synthetic and Systems Biotechnology* **2024,** 9, (2), 340-348.
37. Echeverría, J.; Opazo, J.; Mendoza, L.; Urzúa, A.; Wilkens, M., Structure-activity and lipophilicity relationships of selected Antibacterial natural flavones and flavanones of Chilean flora. *Molecules* **2017,** 22, (4).
38. Koirala, N.; Thuan, N. H.; Ghimire, G. P.; Thang, D. V.; Sohng, J. K., Methylation of flavonoids: Chemical structures, bioactivities, progress and perspectives for biotechnological production. *Enzyme and Microbial Technology* **2016,** 86, 103-116.
39. A., U., DNA Miniprep using CTAB. In 2008.
40. Vandesompele, J.; De Preter, K.; Pattyn, i.; Poppe, B.; Van Roy, N.; De Paepe, A.; Speleman, r., Accurate normalization of real-time quantitative RT-PCR data by geometric averaging of multiple internal control genes. In 2002.
41. Pertea, M., Pertea, G. M., Antonescu, C. M., Chang, T. C., Mendell, J. T., & Salzberg, S. L., StringTie enables improved reconstruction of a transcriptome from RNA-seq reads. *Nature Biotechnology* **2015,** 33, (3), 290–295.
42. Team, R. C. *R: A Language and Environment for Statistical Computing*, v4.3.1; 2025.
43. Mol, J. N. M., Robbins, M.P., Dixon, R.A., Veltkamp, E., Spontaneous and anzymic rearrangement of naringenin chalcone to flavanone. *Phytochemistry* **1985,** 24, (10), 2267-2269.
44. Demarque, D. P.; Crotti, A. E.; Vessecchi, R.; Lopes, J. L.; Lopes, N. P., Fragmentation reactions using electrospray ionization mass spectrometry: an important tool for the structural elucidation and characterization of synthetic and natural products. *Nat Prod Rep* **2016,** 33, (3), 432-55.
45. Jiang, C.; Gates, P. J., Systematic characterisation of the fragmentation of flavonoids using high-resolution accurate mass eectrospray tandem mass spectrometry. *Molecules* **2024,** 29, (22), 5246.
46. Agilent *CrysAlis PRO*, Agilent Technologies Ltd.: Yarnton, Oxfordshire, England, 2014.
47. Farrugia, L., WinGX suite for small-molecule single-crystal crystallography. *Journal of Applied Crystallography* **1999,** 32, (4), 837-838.

 doi:10.20944/preprints202604.2208.v1

48. Sheldrick, G., Crystal structure refinement with SHELXL. *Acta Crystallographica Section C* **2015,** 71, (1), 3-8.
49. Markham, K. R.; Wollenweber, E.; Schilling, G., Structure revision for two *C*-methyl flavanones from *Pityrogramma pallida*. *Journal of Plant Physiology* **1987,** 131, (1), 45-48.
50. Massaro, C. F.; Katouli, M.; Grkovic, T.; Vu, H.; Quinn, R. J.; Heard, T. A.; Carvalho, C.; Manley-Harris, M.; Wallace, H. M.; Brooks, P., Anti-staphylococcal activity of *C*-methyl flavanones from propolis of Australian stingless bees (*Tetragonula carbonaria*) and fruit resins of *Corymbia torelliana* (Myrtaceae). *Fitoterapia* **2014,** 95, 247-57.